Marine Chemistry 110 (2008) 140–152

Contents lists available at ScienceDirect

Marine Chemistry

journal homepage: www.elsevier.com/locate/marchem

Molecular characterization of dissolved organic matter (DOM) along a river to ocean transect of the lower Chesapeake Bay by ultrahigh resolution electrospray ionization Fourier transform ion cyclotron resonance mass spectrometry

Rachel L. Sleighter, Patrick G. Hatcher *

Department of Chemistry and Biochemistry, Old Dominion University, 4541 Hampton Blvd., Norfolk, VA 23529, United States

ARTICLE INFO

Article history:
Received 21 November 2007
Received in revised form 15 April 2008
Accepted 16 April 2008
Available online 26 April 2008

Keywords:
Dissolved organic matter
Mass spectrometry
Estuarine chemistry
Spatial variations
C_{18} solid phase extraction
Chesapeake Bay System

ABSTRACT

In this study, electrospray ionization coupled to Fourier transform ion cyclotron resonance mass spectrometry (ESI-FTICR-MS) is utilized to molecularly characterize DOM as it is transported along a river to estuary to ocean transect of the lower Chesapeake Bay system. The ultrahigh resolving power (greater than 500,000) and mass accuracy of FTICR-MS allow for the resolution of the thousands of components in a single DOM sample, and can therefore elucidate the molecular-level changes that occur during DOM transformation from a terrestrial location to the marine environment. An important feature of FTICR-MS is that its sensitivity allows for direct analysis of low salinity samples without employing the traditional concentration approaches involving C_{18} extraction or ultrafiltration. To evaluate the advantages of using direct analysis, a C_{18} extract of riverine water is compared to its whole, unfractionated water, and it was determined that the C_{18} extraction is selective in that it eliminates two major series of compounds. One group is aliphatic amines/amides that are not adsorbed to the C_{18} disk because they exist as positive ions prior to extraction. The second group is tannin-like compounds with higher oxygen contents and a more polar quality that also allow them not to be adsorbed to the C_{18} disk. This direct approach could not be used for brackish/saline waters, so the C_{18} method is resorted to for those samples. Along the subject transect, a significant difference is observed in the molecular composition of DOM, as determined from assigned molecular formulas. The DOM tends to become more aliphatic and contain lower abundances of oxygen-rich molecules as one progresses from inshore to the offshore. A considerable amount of molecular formula overlap does exist between samples from sites along the transect. This can be explained as either the presence of refractory material that persists throughout the transect, due to its resistance to degradation, or that the assigned molecular formulas are the same but the chemical structures are different. ESI-FTICR-MS is a powerful technique for the investigation of DOM and has the ability to detect compositional variations along the river to ocean transect. Visualization tools such as two dimensional and three dimensional van Krevelen diagrams greatly assist in highlighting the shift from the more aromatic, terrestrial DOM to the more aliphatic, marine DOM.

1. Introduction

Oceanic DOM (a major component of natural organic matter, NOM) is the largest reactive component of the global carbon cycle (Hedges, 1992) and is thought to function as a

* Corresponding author. Tel.: +1 757 683 6537; fax: +1 757 683 4628.
E-mail address: phatcher@odu.edu (P.G. Hatcher).

0304-4203/$ – see front matter © 2008 Elsevier B.V. All rights reserved.
doi:10.1016/j.marchem.2008.04.008

significant short-term sink for atmospheric carbon. The relative reactivity of DOM from numerous sources affects the potential storage capacity and turnover times of this short-term sink, which contains enough reduced carbon that an annual net oxidation of 1% of the supply would generate a CO_2 flux larger than the flux from all anthropogenic sources combined (Hedges, 2002). The global riverine discharge of DOM is adequate to maintain the turnover of the total amount of DOM in the ocean (Williams and Druffel, 1987; Hedges et al., 1997). Although the linking of terrestrial carbon cycles to oceanic carbon cycles through rivers and estuaries is apparent, the amount and composition of that DOM are uncertain. DOM plays an important role in determining the solubility (Chiou et al., 1986, 1987; Fukushima et al., 2006), bioavailability (Traina et al., 1996; Akkanen and Kukkonen, 2003; Akkanen et al., 2004; Gourlay et al., 2005), and eventual fate of associated hydrophobic organic contaminants (Nanny et al., 1997; Nanny and Maza, 2001; Simpson et al., 2004) and trace metals (Sholkovitz, 1978; Sholkovitz et al., 1978; Sholkovitz and Copland, 1981; Santschi et al., 1997; Drexel et al., 2002; Chen et al., 2004). These aspects of DOM imply the necessity for a more fundamental understanding of the chemistry of DOM.

DOM transformation from terrestrial sources to oceanic sources has been the subject of numerous studies (Meyers-Schulte and Hedges, 1986; Coble, 1996; Bianchi et al., 1997; Hopkinson et al., 1998; Repeta et al., 2002; Boyd and Osburn, 2004; Koch et al., 2005; Maie et al., 2005; Meunier et al., 2005; Boehme and Wells, 2006; Tremblay et al., 2007). Samples from many different locations (fresh, brackish/estuarine, marine) have been isolated and concentrated by numerous methods (C_{18} extractions, ultrafiltration, XAD resins), and then analyzed with a variety of chemical and instrumental techniques [lignin-derived phenols as biomarkers, gas chromatography–mass spectrometry (GC–MS), fluorescence excitation-emission matrix (EEM) spectroscopy, bulk elemental analysis, nuclear magnetic resonance (NMR) spectroscopy, and FTICR-MS]. From these studies, it is clear that spatial and seasonal changes can significantly affect DOM's chemical nature and, accordingly, the extent of interactions of DOM with small molecules and estuarine biota. It is well known that terrestrial DOM is more aromatic and contains more carboxyl and hydroxyl functionalities, whereas marine DOM is more aliphatic and is sourced mainly from carbohydrates, amino acids, and lipids. While these bulk characteristics can be easily recognized from various common instruments, the molecular-level characteristics cannot be discerned with conventional analytical techniques. Overall, the chemical and physical changes that occur during DOM transport from river to ocean is a poorly understood process, and here we attempt to elucidate some of these transformations along a river-to-estuary-to-coastal ocean transect of the lower Chesapeake Bay by employing an advanced mass spectrometric approach.

The Chesapeake Bay and its riverine tributaries have been extensively studied in order to better understand how organic matter from sediments (Zimmerman and Canuel, 2000; Arzayus and Canuel, 2004), sediment pore waters (Burdige, 2001; Burdige et al., 2004), particulate organic matter (POM) (Minor and Nallanthamby, 2004; Countway et al., 2007), and DOM (Mitra et al., 2000; Minor et al., 2002; Rochelle-Newall and Fisher, 2002; Minor et al., 2006) contributes to total organic carbon (TOC) and transforms during its export to the bay and eventually the coastal ocean. Mitra et al. (2000) traced lignin sources from the Chesapeake Bay to the Middle Atlantic Bight (MAB) and found that the concentration of lignin phenols in DOM from the Bay was significantly higher than in the MAB. This indicates that DOM from degraded lignin is altered and/or reworked as it travels from its terrestrial source to the marine environment, and it is possible that this portion of refractory DOM is uniformly distributed throughout the ocean. Furthermore, Minor et al. (2006) determined that dissolved inorganic carbon (DIC) increased while DOC and light absorbance decreased after artificial seawater was added to terrestrial DOM and photoirradiated. This incremental addition of seawater to fresh water along with photoexposure simulates the natural transport and mixing of riverine water as it travels to the bay and ocean.

In this study, electrospray ionization coupled to Fourier transform ion cyclotron resonance mass spectrometry (ESI-FTICR-MS) is utilized to detect molecular changes in the composition of five different DOM samples collected along this anthropogenically-impacted estuarine system. The ultra-high resolving power and mass accuracy of FTICR-MS allow for the molecular characterization of DOM, and can, therefore, highlight changes in DOM from various locations (Sleighter and Hatcher, 2007). The details of ESI and FTICR-MS have been described elsewhere (Gaskell, 1997; Marshall et al., 1998). FTICR-MS is the only type of mass spectrometer capable of resolving the exact masses of the thousands of individual components present in a single DOM sample (Llewelyn et al., 2002; Stenson et al., 2002; Kim et al., 2003a; Stenson et al., 2003; Kim et al., 2004; Kramer et al., 2004; Kujawinski et al., 2004; Koch et al., 2005; Hockaday et al., 2006; Kim et al., 2006). With careful calibration, accurate mass to charge (m/z) values can be calculated for each peak, allowing for the determination of molecular formulas that can be confidently assigned with an error of less than 1 ppm (Kujawinski and Behn, 2006). The objectives in this study are to obtain elemental compositions from accurate mass measurements of all peaks observed in the FTICR-MS spectra and to compare the elemental compositions of DOM traversing from inland waters to offshore Chesapeake Bay waters. We specifically attempt to identify the elemental compositions of peaks that are common to inshore and offshore DOM with the prospect that these common components might have a singular source. We also focus on the elemental compositions of peaks that are uniquely observed in each of the inshore or offshore DOM samples to elaborate on possible sources for such components.

2. Experimental

2.1. Samples and preparation

Water sampling begins at the Great Dismal Swamp in southeastern Virginia, continues north up the Elizabeth River to the Chesapeake Bay, and concludes approximately 10 miles off the coast in the Atlantic Ocean (Fig. 1). Site #1 is in the Great Dismal Swamp (Suffolk, Virginia) and represents the swampy, highly terrestrial DOM headwaters of the Elizabeth River system. Site #2 (Great Bridge, Virginia) is the up-river site and its shore is lined with marshes. Site #3 (Norfolk, Virginia) is the mid-river site that includes not only autochthonous and allochthonous organic matter from the three branches of the Elizabeth River and lower Chesapeake Bay, but also anthropogenic contributions from downtown Norfolk and Portsmouth. Site #4 (the Chesapeake Bay Bridge-Tunnel, Virginia) is the down-river site where

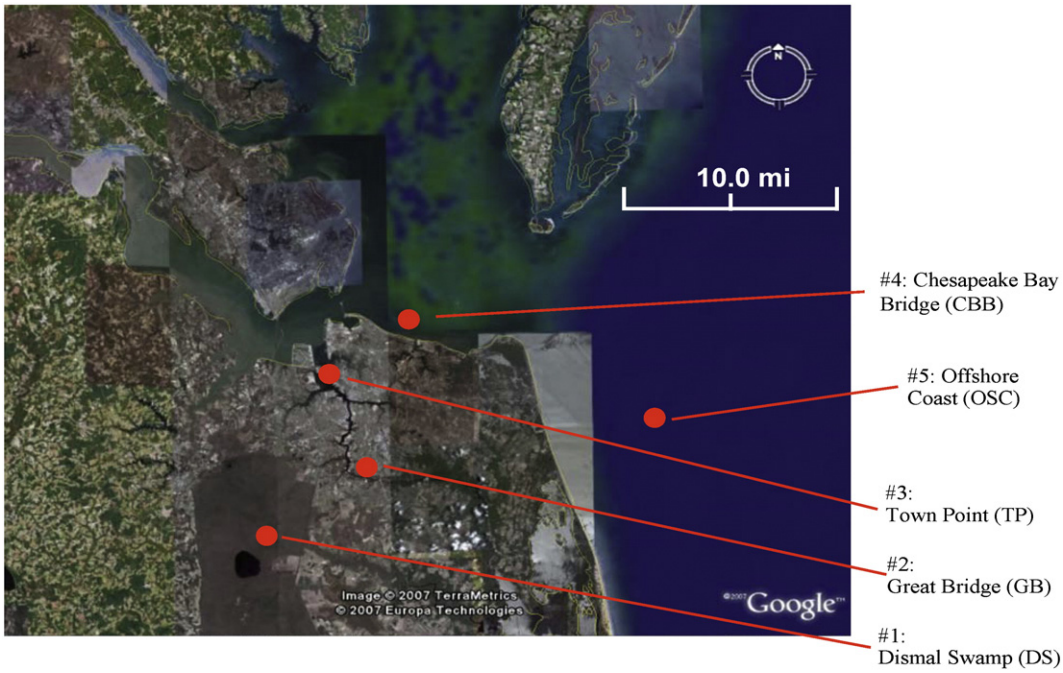

Fig. 1. Satellite image of the lower Chesapeake Bay and environs showing the five sampling sites along the terrestrial to marine transect. Sampling site abbreviations are shown in parentheses. Image provided, with permission, by Google Earth™ mapping service.

the Chesapeake Bay mouth opens to the Atlantic Ocean. This site has organic matter sources from the salt marshes and sediments from the lower Chesapeake Bay and its estuaries, marine material imported from the coast, and autochthonous algal production. Site #5 is the offshore coastal ocean site, which is approximately 10 miles off the coast and contains autochthonous marine organic matter as well as any terrestrial organic matter that survives transport from the river to the ocean. Water from this site was obtained while on board the R/V Fay Slover, a research vessel owned and operated by Old Dominion University.

Surface water was collected from each site in November 2006, and ambient temperature, salinity, and pH were immediately measured. The whole water was filtered through a 0.1 μm Whatman Polycap cartridge filter to remove bacteria and particulates, and DOC concentrations were determined afterwards on an Aurora 1030W TOC Analyzer (wet oxidation) instrument. Dissolved inorganic carbon (DIC) was removed prior to DOC analysis by acidifying samples to a pH of 2. Table 1 displays the various properties (i.e., DOC, pH, salinity, temperature) that were measured for water at each site. As one travels along the transect, the pH and salinity increase while the DOC decreases. The natural presence of organic acids is responsible for the low pH in the Dismal Swamp (Lichter and Walker, 1979; Johannesson et al., 2004), and the DOC decline is due to dilution and mixing with lower DOC waters in the Chesapeake Bay system.

DOM was isolated from the water samples from all five sites using C_{18} solid phase extraction disks (3M, Empore) using previously established protocols (Kim et al., 2003b). The primary goal was to analyze the DOM by ESI-FTICR-MS, which requires a very low salt content. The C_{18} methodology provides an efficient process for desalting brackish and marine samples. Because the Dismal Swamp water has a high ambient DOC concentration and zero salinity, it was also analyzed without the C_{18} extraction protocol. The C_{18} disks were activated using LC-MS grade water and methanol (Fisher Scientific), and each water sample was acidified to a pH of 2 before passing through the disk. The amount of sample passed through each C_{18} disk varied with the ambient concentration of DOC. Approximately 0.25 L of Dismal Swamp water, 0.5 L of Great Bridge and Town Point water, 1 L of Chesapeake Bay Bridge water, and 2 L of offshore coastal water were extracted. The adsorbed material was rinsed with LC-MS grade water before eluting off the disk with LC-MS grade methanol. Dismal Swamp DOM was eluted with 20 mL of methanol, while 4 mL was used for Great Bridge and Town Point DOM and 2 mL of methanol was used for Chesapeake Bay Bridge and offshore coastal DOM. Due to the qualitative nature of these studies, the recovery from the C_{18} disk was not measured. Previous studies have shown that approximately 42%–60% of riverine DOM is recovered by this technique (Louchouarn et al., 2000; Kim et al., 2003b), while 32% of estuarine DOM and 22% of marine DOM could be recovered (Louchouarn et al., 2000). The two separate mass spectral analyses of Dismal Swamp whole water and C_{18} extracted Dismal Swamp water will also determine if the C_{18} isolated material is representative of the whole.

2.2. Instrumentation

The C_{18} extracted samples were diluted with LC-MS grade water, while the Dismal Swamp whole water, without C_{18} extraction, was diluted with LC-MS grade methanol, to give a final sample composition of 50:50 (v/v) methanol:water for all samples. In order to increase the ionization efficiency, ammonium hydroxide was added immediately prior to ESI, bringing the pH up to 8. Before analyzing the C_{18} extracted DOM samples, a blank of 50:50 (v/v) methanol:water with 0.1% ammonium hydroxide was analyzed on the FTICR-MS, and these blank analyses confirmed that there was no contamination from previous samples. Samples were continuously infused into an Apollo II ESI ion source of a Bruker Daltonics 12 Tesla Apex Qe FTICR-MS, housed at the College of Sciences Major Instrumentation Cluster (COSMIC) at Old Dominion University. Samples were introduced by a syringe pump providing an infusion rate of 120 μL/h. All samples were analyzed in negative ion mode, and electrospray voltages were optimized for each sample. Previous studies show that negative ion mode avoids the complications of the positive ion mode in which alkali metal adducts, mainly Na^+, are observed along with protonated ions (Brown and Rice, 2000; Rostad and Leenheer, 2004). Ions were

Table 1
Properties measured for each site along the transect

Site	Temperature (°C)	pH	Salinity	DOC (ppm C)[a]
Dismal Swamp (DS)	11.8	3.30	0	136.2±1.1
Great Bridge (GB)	15.0	7.13	11	10.28±0.19
Town Point (TP)	14.3	7.21	20	5.26±0.02
Chesapeake Bay Bridge (CBB)	15.4	7.51	22	3.37±0.17
Off Shore Coast (OSC)	16.2	8.01	32	2.27±0.06

[a]Error is the standard deviation of three measurements.

accumulated in a hexapole for 1.0 s before being transferred to the ICR cell. Exactly 200 transients, collected with a 4 MWord time domain, were added, giving about a 20 min total run time. The summed free induction decay (FID) signal was zero-filled once and sine-bell apodized prior to fast Fourier transformation and magnitude calculation using the Bruker Daltonics Data Analysis software.

2.3. Mass calibration and molecular formula assignments

Prior to data analysis, all samples were externally calibrated with an arginine cluster standard and internally calibrated with a new method that adventitiously calibrates with fatty acids naturally present within the sample (Sleighter et al., 2008). Fatty acids, mainly those with carbon chain lengths of C_{14}–C_{32} are ubiquitous components of DOM (Slowey et al., 1962; Kaiser et al., 2003; Mannino and Harvey, 1999; Mannino and Harvey, 2000; Minor et al., 2001; Frazier et al., 2005; McCallister et al., 2006), and because they charge readily in negative ionization mode (Henriksen et al., 2005), they are ideal for use as internal calibrants. A molecular formula calculator developed at the National High Magnetic Field Laboratory in Tallahassee, FL, (Molecular Formula Calc v.1.0 ©NHMFL, 1998) generated empirical formula matches using carbon, hydrogen, oxygen, nitrogen, sulfur, and phosphorus. Only m/z values with a signal to noise above 5 were inserted into the molecular formula calculator. The assigned formulas, in the vast majority of cases, agreed within an error value of less than 0.5 ppm when compared to the calculated exact mass of the determined formulas.

3. Results and discussion

3.1. General spectral characteristics of C_{18} extracted DOM

As examples of the spectra obtained in this study, Fig. 2a and b shows the negative ion mass spectra of the C_{18} extracted Dismal Swamp water and the C_{18} extracted offshore coastal water, respectively. The DOM mass spectra consist of a multitude of peaks spanning the m/z range of 200–700, and complexity is apparent from the detection of up to 15 peaks per nominal mass at nearly every mass throughout that range. The majority of peaks appears at odd m/z values, and based upon the nitrogen rule, indicate a predominance of zero or an even number of nitrogens in the molecules. From the expanded insets of Fig. 2, one can note that the peaks are singly charged due to the observation of the isotopic peaks at 1.00335 m/z units (the mass of a neutron) higher than the parent peak. This is the case for the entire mass range, indicating that all peaks are singly charged, which is similar to previous findings for DOM (Kujawinski et al., 2002; Stenson et al., 2002; Kim et al., 2003a). Resolving power is the exact mass of the peak divided by the full width at the half maximum of that peak. The average broadband resolving powers of these mass spectra exceeded 580,000 and individual peak resolving powers at the center of the m/z range, m/z 401, exceeded 725,000.

There are multiple orders of fine structure in the mass spectra shown in Fig. 2. One of these is the observation of low m/z peaks that stand out above all others in the spectra. These peaks, at m/z 255.23295, 281.24806, and 283.26424, originate from the C_{16} saturated fatty acid, the C_{18}:1 unsaturated fatty acid, and the C_{18} saturated fatty acid, respectively. As previously mentioned in Section 2.3, fatty acids have very high ionization efficiencies that lead to their increased peak magnitude, which is not necessarily proportional to their actual concentration. Two other large peaks, at 368.97651 and 412.96638 are artifacts from the C_{18} extraction and are present in all C_{18} extracted samples. Another observation is the repeating patterns every 14.01566 mass units, which indicates the incremental addition of a CH_2 group. At every nominal mass, up to three different series of peaks differing by 0.03641 m/z units are observed. This mass difference equates to the replacement of one oxygen atom with a CH_4, and has been noted in previous mass spectra of DOM (Stenson et al., 2003). The large clusters of peaks at 600–603 m/z and 671–674 m/z in the offshore coastal sample are chlorine adducts, determined primarily from isotope patterns and matches to exact masses. In this case, the analyte becomes chlorinated, presumably from trace amounts of chloride ions not removed by the C_{18} extraction. In general, the intricacies of each mass spectrum are not apparent when viewing its full spectral range, simply due to the complex nature of DOM. It is from expanded regions of the spectra that one can better assess changes that occur from one sample to the next. However, prior to a more critical examination of the spectra along this transect, it is pertinent to discuss the influence C_{18} extraction has on spectral characteristics. Obtaining a mass spectrum by directly infusing whole water from the Dismal Swamp and comparing it with C_{18} extracted Dismal Swamp water allows for the evaluation of the molecular fractionation inherent in the C_{18} method commonly used for ESI-FTICR-MS analysis of DOM.

3.2. Efficacy of the C_{18} extraction for DOM characterization

Fig. 3a and b shows the negative ion mass spectra of the C_{18} extracted Dismal Swamp water and the Dismal Swamp whole water, respectively. The

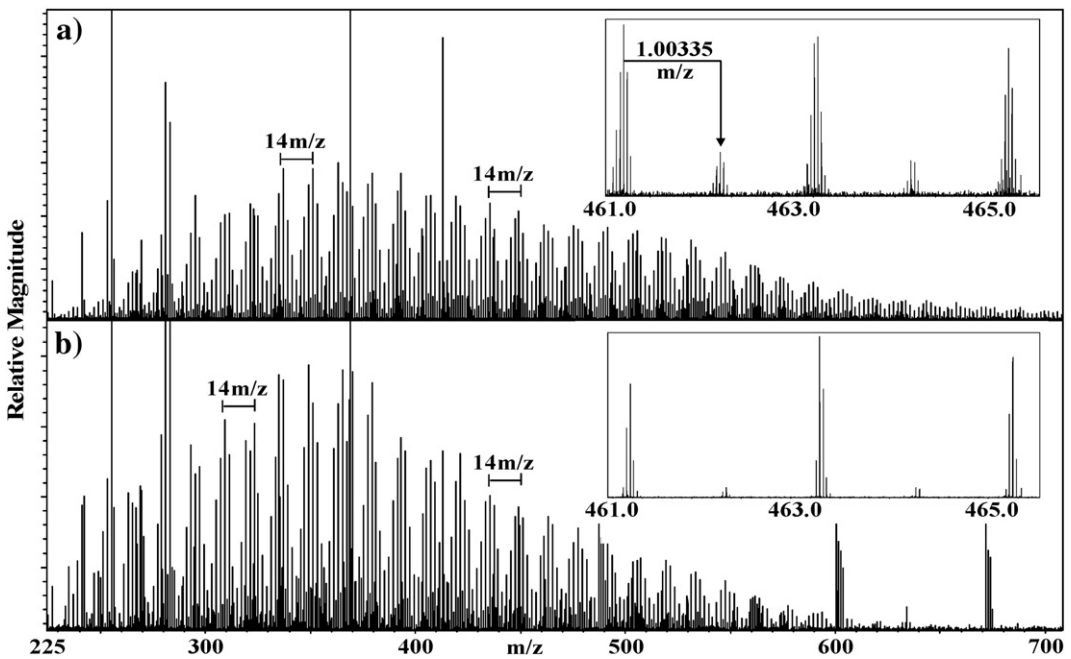

Fig. 2. a) Negative ion mass spectrum (m/z 200–700) of C_{18} extracted Dismal Swamp water. b) Negative ion mass spectrum (m/z 200–700) of C_{18} extracted offshore coastal water. The insets are an expanded region of 461.0–465.5, to highlight the complexity at each nominal mass and to show that the analytes are singly charged.

large peaks in the *m*/*z* range of 225–300 in the whole water mass spectrum are assigned to fatty acids (saturated and unsaturated). Fatty acid peaks do not appear as abundant in the C_{18} extracted DOM (Fig. 3a). Clearly, the C_{18} extraction has fractionated the proportions of fatty acids relative to other non-fatty acid components. Large peaks at *m*/*z* 368.97651 and 412.96638, derived from the C_{18} disk, are not observed in the whole water. The insets of Fig. 3a and b emphasize the difference between the two samples in a narrow, nominal mass window, a difference that is noted at nearly every odd nominal mass region throughout the mass spectra. The peaks at a low mass defect in the whole water spectrum are not observed in the C_{18} extract. Low mass defect species (peaks existing at up to 0.15 mass units from the exact nominal mass) are indicative of compounds with a high oxygen content and/or a low hydrogen content (Kim et al., 2003a). Oxygen, with an exact mass of 15.994915, imparts a negative mass defect, while hydrogen, with an exact mass of 1.007825, imparts a positive mass defect. The increased number of oxygens associated with molecules responsible for these peaks likely amplifies polarity or hydrophilicity, which limits their absorptivity onto the C_{18} disk.

Additional information about the types of compounds lost during C_{18} extractions can be determined by assigning molecular formulas to the peaks in each spectrum. Assignments are made using the molecular formula calculator, described above in Section 2.3, and functional group relationships, as revealed by Kendrick mass defect (KMD) analysis (Kendrick, 1963; Stenson et al., 2003; Kujawinski and Behn, 2006), assist in confidently assigning formulas. By using the formula extension approach, described by Kujawinski and Behn (2006), higher *m*/*z* peaks were assigned a molecular formula based on a relationship to a lower *m*/*z* peak. Because heteroatoms were allowed in the formula calculator (N, S, and P), the following conservative ratios were applied when assigning molecular formulas: N/C<0.5, S/C<0.2, P/C<0.1, and (S+P)/C<0.2. Once all molecular formulas are assigned with confidence, van Krevelen (VK) diagrams (van Krevelen, 1950; Kim et al., 2003a; Hertkorn et al., 2007) are constructed to elucidate differences between the mass spectra. The VK diagram plots the molar H/C ratios on the *y*-axis and the molar O/C ratios on the *x*-axis, and is utilized to assist in clustering molecules according to their functional group compositions. The unique O/C and H/C ratios for each formula align and fall at a certain point on the diagram, reflective of the type of molecule. This visualization tool not only identifies what types of compounds are present in the sample, but also highlights variations between samples by overlaying numerous plots.

Fig. 4a shows the VK diagram of the Dismal Swamp whole water overlain with that of the C_{18} extracted Dismal Swamp water. The points in red denote formulas for peaks that appear in both the Dismal Swamp whole water and the C_{18} extracted Dismal Swamp water, whereas points in blue are from formulas of peaks that appear in the whole water only. Major compound classes are emphasized within the circles on the plot. Fig. 4b shows points that appear only in the Dismal Swamp whole water, colored according to their relative peak magnitude (i.e., percentage of the summed total peak magnitude). The first major difference in the two VK plots of Fig. 4a is the abundance of points that appear at a high O/C ratio (0.65–0.95) in the Dismal Swamp whole water. These points correspond to the low mass defect species that are present only in the whole water mass spectrum (Fig. 3), and they plot in the tannin region of the diagram. Tannins, which occur in higher plants and some algae, are polyphenolic compounds that contain a variety of linkages and central cores (De Leeuw and Largeau, 1993). It is estimated that tannin-like substances account for approximately 14% of the summed total peak magnitude in the Dismal Swamp whole water. No other VK diagrams of DOM containing such high O/C ratios, to our knowledge, have been published, in large part because previous investigators have been unable to obtain ESI-FTICR-MS spectra directly of whole, untreated water.

Another VK diagram plot region for the Dismal Swamp whole water that is not represented by an abundance of peaks in the C_{18} extract is the aliphatic amines/amides region. Samples are acidified to a pH of 2 prior to extraction in order to protonate any sites with a negative charge, but it also fully protonates nitrogen atoms, leading to the formation of a water-soluble cationic species. The cationic compounds pass through the C_{18} disk, as they are hydrophilic and tend not to be adsorbed to the hydrophobic C_{18}. These aliphatic nitrogenous species account for approximately 8% of the summed total peak magnitude in the Dismal Swamp whole water. This agrees well with a recent study of marine DOM, where an abundance of nitrogen-containing organic molecules was detected by FTICR-MS in an isolated hydrophilic fraction (Reemtsma et al., 2008). Approximately 22% of the summed total peak magnitude is due to aliphatic nitrogenous compounds and tannin-like compounds, which accounts for about half of the missing extraction efficiency of the C_{18} disk reported above in Section 2.1. The C_{18} extraction methodology, being the standard protocol in many ESI-FTICR-MS studies of DOM (Kim et al., 2003a,b, 2004; Kujawinski et al., 2004; Koch et al., 2005; Dittmar and Koch, 2006; Hockaday et al., 2006; Kim et al., 2006; Tremblay et al., 2007), obviously discriminates against oxygen-rich tannin-like substances and nitrogenous species.

While recognizing that ESI-FTICR-MS is not a quantitative technique, the relative magnitudes of the various peaks and the molecular formulas they represent can, nonetheless, be calculated and compared. As shown in Fig. 5, 97.4% of the magnitude-weighted formulas in the C_{18} extracted Dismal Swamp water contain only the elements CHO, and these formulas are less diverse than those in the Dismal Swamp whole water which contain 83.3% of CHO-only groups. The total percentage of any compound containing nitrogen

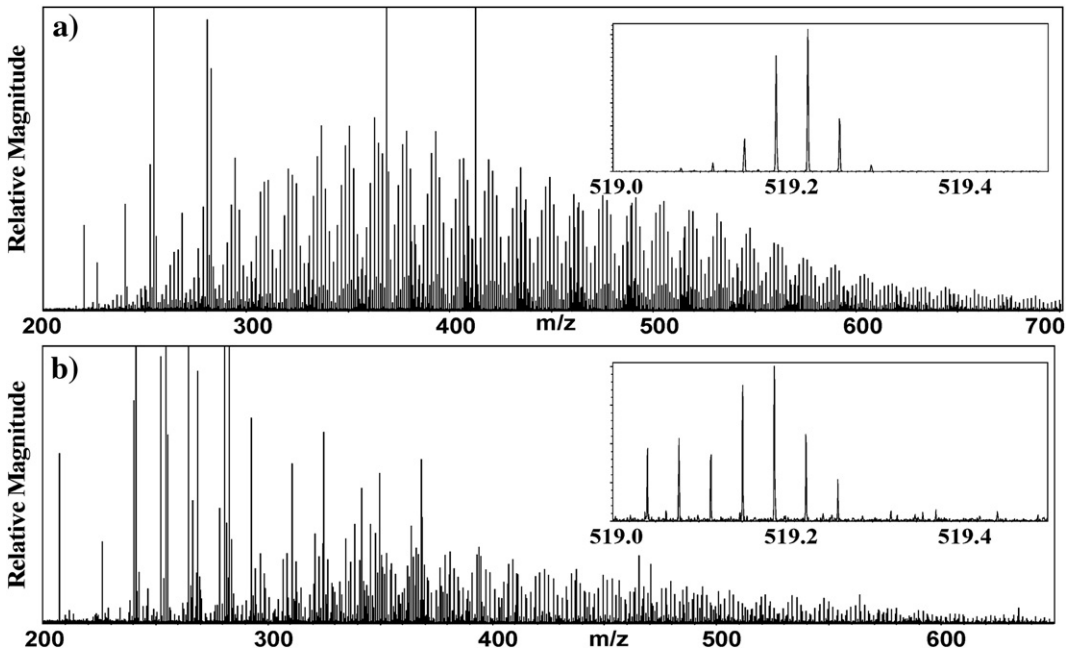

Fig. 3. a) Negative ion mass spectrum (*m*/*z* 200–700) of C_{18} extracted Dismal Swamp water. b) Negative ion mass spectrum (*m*/*z* 200–650) of the Dismal Swamp whole water. The insets are an expanded region of nominal mass 519, to highlight the low mass defect species that exist in the whole water but not the C_{18} extract.

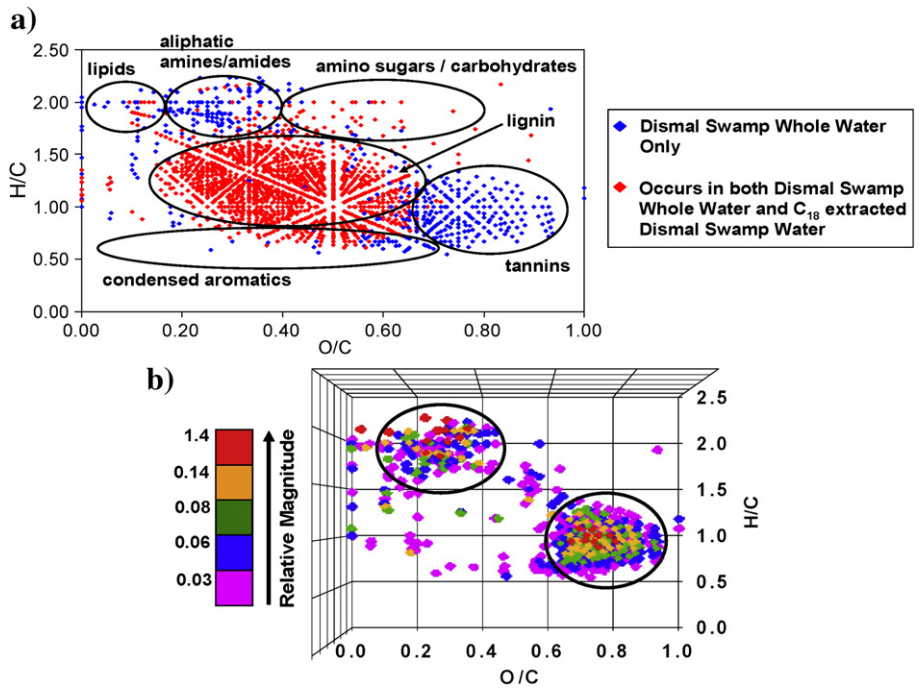

Fig. 4. a) The van Krevelen diagram of the Dismal Swamp whole water overlain with the C_{18} extracted Dismal Swamp DOM. b) The van Krevelen diagram of peaks appearing in the Dismal Swamp whole water that are not present in the C_{18} extracted Dismal Swamp DOM, color coded according to relative peak magnitude (percent of the summed total peak magnitude). The magnitudes increase in the order pink, blue, green, orange and red. Circles on this plot indicate the two major regions of difference between the Dismal Swamp whole water and the C_{18} extracted Dismal Swamp DOM.

is 1.4% and 9.4% for the C_{18} extracted Dismal Swamp water and the Dismal Swamp whole water, respectively, which clearly demonstrates the bias against nitrogenous compounds when using C_{18} extraction. The presence of peaks containing CHO and other atoms such as sulfur and phosphorus is also less apparent in C_{18} extracted Dismal Swamp water. It therefore appears that the C_{18} preferentially extracts CHO compounds, while discriminating against the more polar compounds with heteroatom functionalities.

From the molecular formula assignments, the magnitude-averaged O/C, H/C, and double bond equivalent (DBE) values for each sample can be determined by the following formulas:

$$(O/C)_w = \Sigma(O/C_n * M_n)$$
$$(H/C)_w = \Sigma(H/C_n * M_n)$$
$$DBE = 1/2*(2\#C + \#N + \#P - \#H + 2)$$
$$(DBE)_w = \Sigma(DBE_n * M_n)$$

where *w* signifies a magnitude-weighted calculation, *n* signifies that the parameter is calculated for each assigned molecular formula, # represents the number of the specified atoms in the molecular formula, and *M* is the relative magnitude of each peak. The Dismal Swamp whole water has magnitude-averaged O/C_w, H/C_w, and DBE_w values of 0.44, 1.34, and 7.6, respectively. The C_{18} extracted Dismal Swamp water has magnitude-averaged O/C, H/C, and DBE values of 0.39, 1.25, and 9.6, respectively. The more oxygenated compounds that are emphasized in Fig. 4 (those not retained by the C_{18} disk) not only elevate the average O/C value but they also diminish the DBE.

In summary, we have shown how C_{18} extractions can fractionate DOM from the Dismal Swamp and eliminate certain groups of compounds from the analysis. It is thought that the C_{18} procedure similarly fractionates all other samples of DOM as well. Although previous studies utilizing the C_{18} extraction protocol may have considered the hydrophobic portion of the DOM to be representative of the whole, the least invasive sample preparation (e.g., direct infusion into the mass spectrometer) will always lead to the more extensive characterization of any DOM sample. We fully recognize that there is an inherent discrimination when using C_{18} disks as an extraction method, but the presence of salts in brackish/saline samples from along the transect prevents direct mass spectral analysis at this time. Electrospray ion sources are very sensitive to salts (Stenson et al., 2002), so the C_{18} technique is

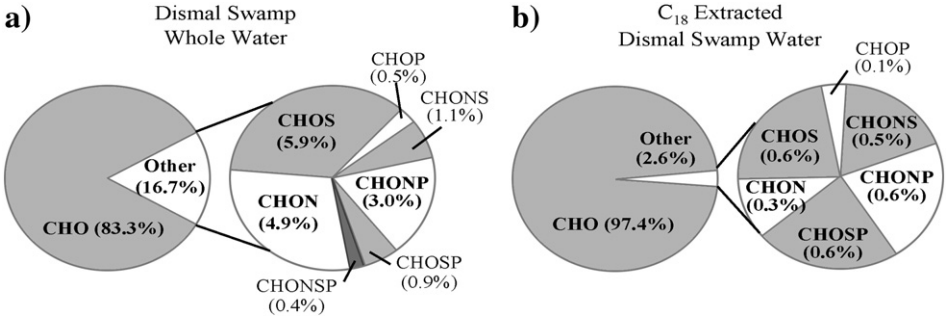

Fig. 5. Pie charts of the percentages (magnitude-weighted) of each type of molecular formula present in Dismal Swamp whole water (a) and C_{18} extracted Dismal Swamp water (b).

resorted to for comparison of all samples, acknowledging that each sample would be biased in the same manner.

3.3. Spatial variations in DOM along the transect

As mentioned previously in Section 3.1, comparing the full mass range for the mass spectra is not particularly informative, so the ensuing discussion focuses on expanded regions of the spectra meant to demonstrate general trends among the 5 samples in the transect. Fig. 6 shows expanded regions at nominal m/z values of 315, 427, 483, and 519 of the C_{18} extracted Dismal Swamp water (Fig. 6a) and the C_{18} extracted offshore coastal water (Fig. 6b). Only data for the two extremes of the transect are shown for the sake of clarity. These are obtained from the full mass spectra shown in Fig. 2, and the mass ranges are selected randomly only to indicate shifts in mass defect observed at each nominal mass across the entire spectral range. Over the entire mass range, there is considerable similarity between peaks observed in the Dismal Swamp and offshore DOM samples. Many peaks are present in all samples, but some significant shifts in the relative magnitudes are apparent. Peaks that exist in both samples that are assigned identical molecular formulas could imply that the same compounds are present in both samples. However, this is probably not the case because each peak representing an exact formula could comprise a multitude of structural entities having the same elemental composition and exact mass. Full resolution of structural similarities will require MS/MS characterization of each peak, a capability that is not yet possible for these types of complex samples.

As DOM is exported through the river system to the coastal ocean, there is a shift in the relative magnitude of peaks that are of similar exact mass. For example, when comparing the same nominal mass region between these two samples (as shown in Fig. 6), the larger peak magnitude shifts from low mass defect peaks to those of higher mass defect. Using nominal mass 427 as an example, the highest magnitude peak in the envelope for the C_{18} extracted Dismal Swamp water is at m/z 427.13994, while the highest magnitude peak in this envelope for the C_{18} extracted offshore coastal water is at m/z 427.19726. For each DOM sample, the peak magnitude relationships are nearly identical from one nominal mass region to the next. However, when comparing the same nominal mass between these two samples, the higher magnitudes shift to the high mass defect species in each respective nominal mass. The other striking difference between onshore and offshore samples is that peaks at low mass defect in each envelope disappear altogether as sampling progresses offshore, with new peaks at high mass defect emerging in the offshore sample. This trend is also observed in the Kendrick mass defect plots (not shown); the offshore samples have more peaks with high KMD values while inshore samples have an abundance of peaks with low KMD values. This shift of peak magnitude within each nominal mass indicates that the organic matter from the offshore site is oxygen poor and/or hydrogen rich when compared to the onshore sample from the Dismal Swamp, consistent with the notion that terrestrial organic matter is perhaps more aromatic while marine organic matter is likely to be more aliphatic.

In addition to the two dimensional VK diagram shown in Fig. 4a, one can also display the information in three dimensions by adding ion magnitude or another molar ratio (N/C, S/C, etc.) as the z-axis. Plotting relative ion magnitude as the third dimension provides an indication of which compound class is in highest abundance, but because ionization efficiency plays a large role in determining the ion's plotted magnitude, this comparison should only be used qualitatively. For simplicity, only the two end-members of the transect are shown here, even though trends are observed that grade consistently from one site to the next. Fig. 7 shows the three dimensional VK diagrams for C_{18} extracted Dismal Swamp water and the C_{18} extracted offshore coastal water. The most noticeable comparison among these plots is their remarkable similarity. The offshore sample appears to display a more confined distribution than the Dismal Swamp sample, but in both samples, the major peak magnitudes lie in a region assigned to lignin-derived molecules. There is a small shift in the maximum of the distribution towards higher H/C and lower O/C ratios, which is characteristic of a shift to more aliphatic structures in the offshore sample. This trend simply reflects what was previously discussed: that the offshore sample contains more H-rich, O-poor compounds. However, it is clear that the peaks with the highest relative magnitudes (shown in red) in both samples have approximately the same elemental compositions. It may appear that the lower intensity peaks only exist along the outer edge of the cluster, but if peaks are plotted with only those of similar magnitude on this type of plot (i.e., only peaks of the same color code), the peaks all cluster within the same region as observed for the most intense peaks. This exercise was done to convince ourselves that peaks of lower magnitude were only being masked by those of higher magnitude on the plots in Fig. 7. Furthermore, the magnitude-averaged O/C_w, H/C_w, and DBE_w values were calculated for each set of relative magnitudes (i.e., each color code), and these calculated values were found to be statistically the same among each color code, for the two DOM samples.

Table 2, showing the calculated magnitude-averaged O/C_w, H/C_w, and DBE_w values of all five samples, illustrates the molecular-level changes that occur as DOM is transported from the terrestrial Dismal Swamp to the

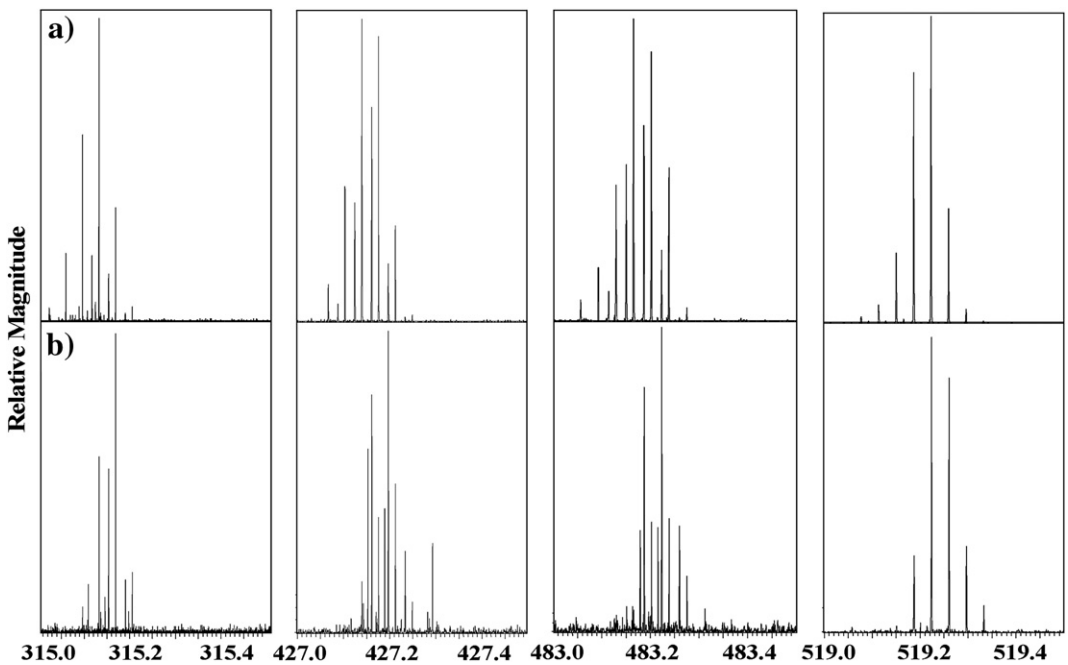

Fig. 6. Negative ion mass spectra expanded at nominal masses 315, 427, 483, and 519 of C_{18} extracted Dismal Swamp water (a) and C_{18} extracted offshore coastal water (b). Although many peaks appear in both samples, a shift in relative magnitude from low mass defect to high mass defect is observed.

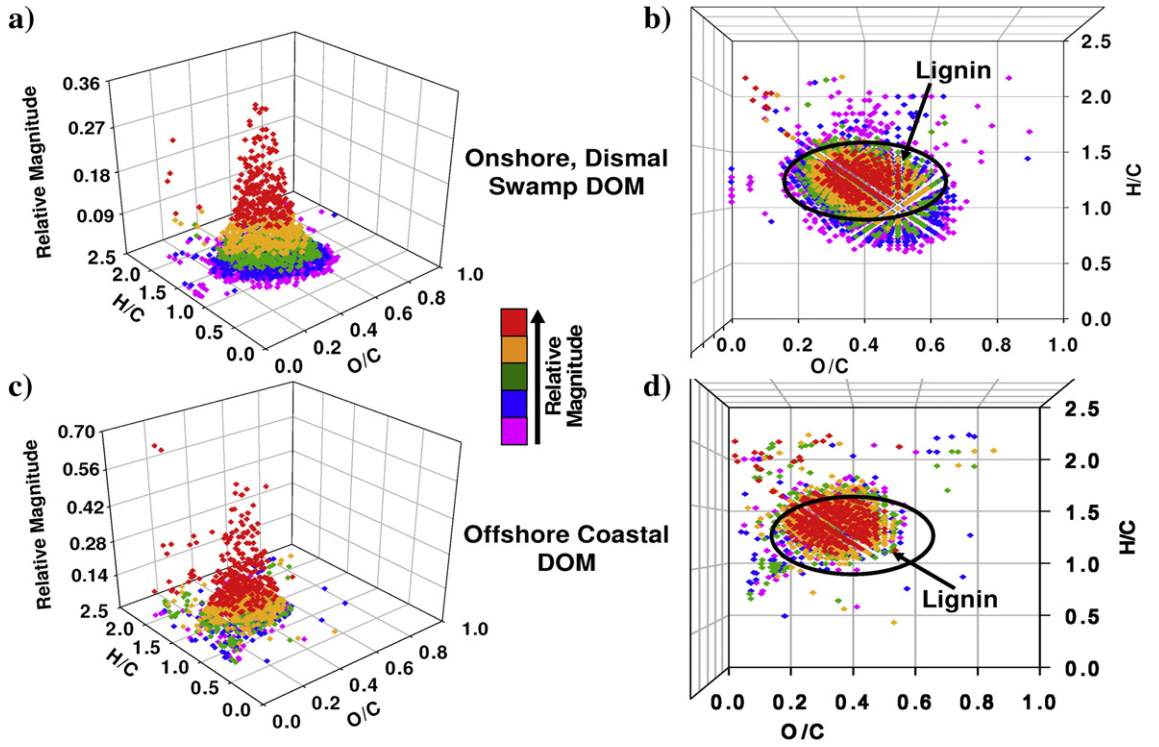

Fig. 7. The three dimensional van Krevelen diagrams of the C_{18} extracted Dismal Swamp water (a and b) and the C_{18} extracted offshore coastal water (c and d) created by adding the relative peak magnitudes (percent of the summed total magnitude) as the *z*-axis (a and c) alongside color coded plain views (b and d). The magnitudes increase in the order pink, blue, green, orange and red.

estuarine environment of the Chesapeake Bay and then to the Atlantic Ocean. The main observation is the increase in H/C with a concomitant decrease in DBE, indicating that the characteristics of each DOM sample transform such that the molecules become more saturated as one progresses offshore. Although the O/C ratio initially decreases upon leaving the Dismal Swamp, it does not significantly change along the transect. Another trend observed is that DOM becomes more chemically diverse offshore, as depicted in Fig. 8 where the relative proportions of compounds containing elements other than C, H, and O are depicted. The compounds with only CHO formulas decrease in magnitude while compounds containing nitrogen, sulfur, and phosphorus functionalities increase in magnitude. Although CHO-only formulas are the major contributors to the peak magnitude, as one progresses offshore, the heteroatom functionality significantly increases from 2.6%–16.3%.

To examine the nature of this increased heteroatom functionality, it is important to investigate the types of structures containing N, S, and P. By plotting the peaks of compounds which contain N, S, and P on a three-dimensional VK diagram, it is possible to examine what types of molecules are present and their relative magnitude (Fig. 9). In the C_{18} extracted Dismal Swamp water, the compounds containing N and S (Fig. 9a and b) are present in very low relative magnitude and seem to be randomly distributed across the entire plot. In the C_{18} extracted offshore coastal water, there are two clusters in the plot of S-containing compounds: one in the lipid region and one to the left of the lignin region (Fig. 9b). Because these S-containing formulas cannot be assigned to any type of oxidized or reduced sulfur species at this time, speculation as to their source is unwarranted.

In both samples, the phosphorus-containing peaks (Fig. 9c) plot near the reported lipid region, but are shifted slightly to the right. These peaks are characteristic of phospholipids, and the higher oxygen content of a phosphate group shifts the cluster of points to the higher O/C ratio. It is very likely that the DOM in the offshore sample has a significant contribution from autochthonously-produced cell membranes that are comprised of phospholipid molecules, where typically the hydrophobic end is linked to the hydrophilic end through a phosphodiester bond (Nelson and Cox, 2000b). The nitrogen-containing peaks in the C_{18} extracted offshore coastal water cluster in a region that is slightly below the phospholipids on the VK plot. Some of the peaks assigned to phospholipids also contain nitrogen, which is not uncommon because glycerophospholipids contain an amine functionality in their polar head-group (Nelson and Cox, 2000b). There is also a small cluster of phosphorus-containing peaks in the carbohydrate region of the plot. During carbohydrate synthesis and metabolism within a cell, intermediates are often phosphorylated, with a phosphoric acid condensing with one of the hydroxyl groups to form a phosphate ester (Nelson and Cox, 2000a). Overall, offshore DOM is comprised of molecules that seem to be mainly derived from autochthonous primary production and these tend to have more N, S, and P atoms incorporated into the organic matter. In contrast, the primary source of DOM from Dismal Swamp is terrestrial vegetation, and there is very little algal growth due to the low pH and limited light penetration.

Even though the mass spectra and VK diagrams show an overall significant shift in the types of compounds present in the various samples along the transect, there is a considerable similarity among the samples. Fig. 10 shows a Venn diagram for the overlap of molecular formulas for the C_{18} extracted samples of Dismal Swamp water (terrestrial inputs), Town Point water (central site), and offshore coastal water (marine inputs). In areas of no overlap, percentages are of the molecular formulas that are unique to that site. In areas where there is overlap, percentages represent the number of molecular formulas that are found in both (or all three) of those sites. The Dismal Swamp contains the largest number of compounds with unique formulas (32%) while the Town Point sample has the least (5%). Town Point, being the central site with the most exchange from both end-members, overlaps more significantly with both the Dismal Swamp site and the

Table 2
Magnitude-averaged O/C_w, H/C_w, and DBE_w values for each site along the transect

DOM Sample	O/C_w	H/C_w	DBE_w
C_{18} extracted Dismal Swamp water	0.39	1.25	9.6
C_{18} extracted Great Bridge water	0.35	1.29	8.5
C_{18} extracted Town Point water	0.35	1.37	7.6
C_{18} extracted Chesapeake Bay Bridge water	0.35	1.40	7.4
C_{18} extracted Offshore Coastal water	0.33	1.43	7.2

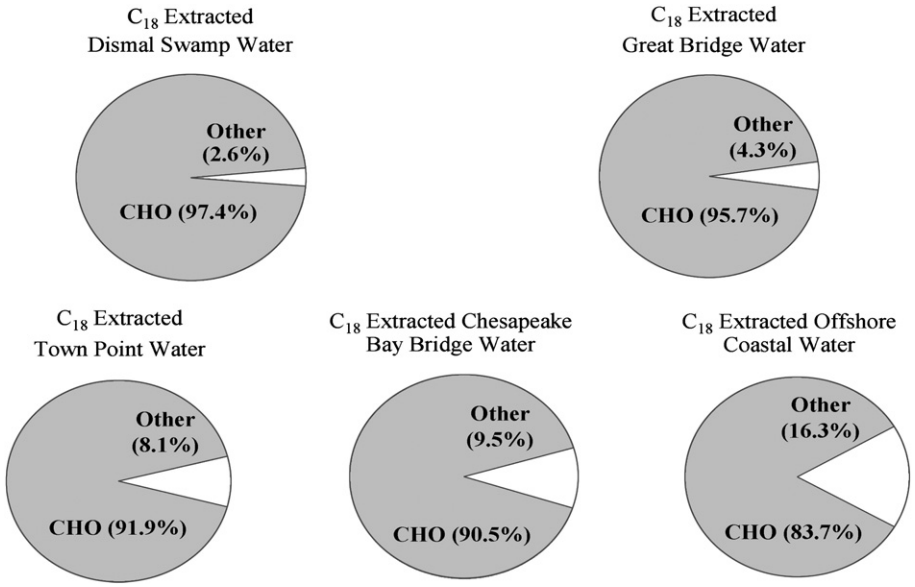

Fig. 8. Pie charts showing the percentages (magnitude-weighted) of CHO-only molecular formulas present in the C_{18} extracts of each sampling site along the transect. Other refers to molecular formulas containing C, H, O, along with other atoms as well (N, S, and P).

offshore coastal site than the Dismal Swamp with the offshore coastal site. Of all the overlapping peaks, the largest percentage is from peaks that are common to all of the samples (29%), which suggest an inherently similar material or formula that exists in all of the samples. However, one should keep in mind that simply because the molecular formulas match, this does not mean that the actual structures also match.

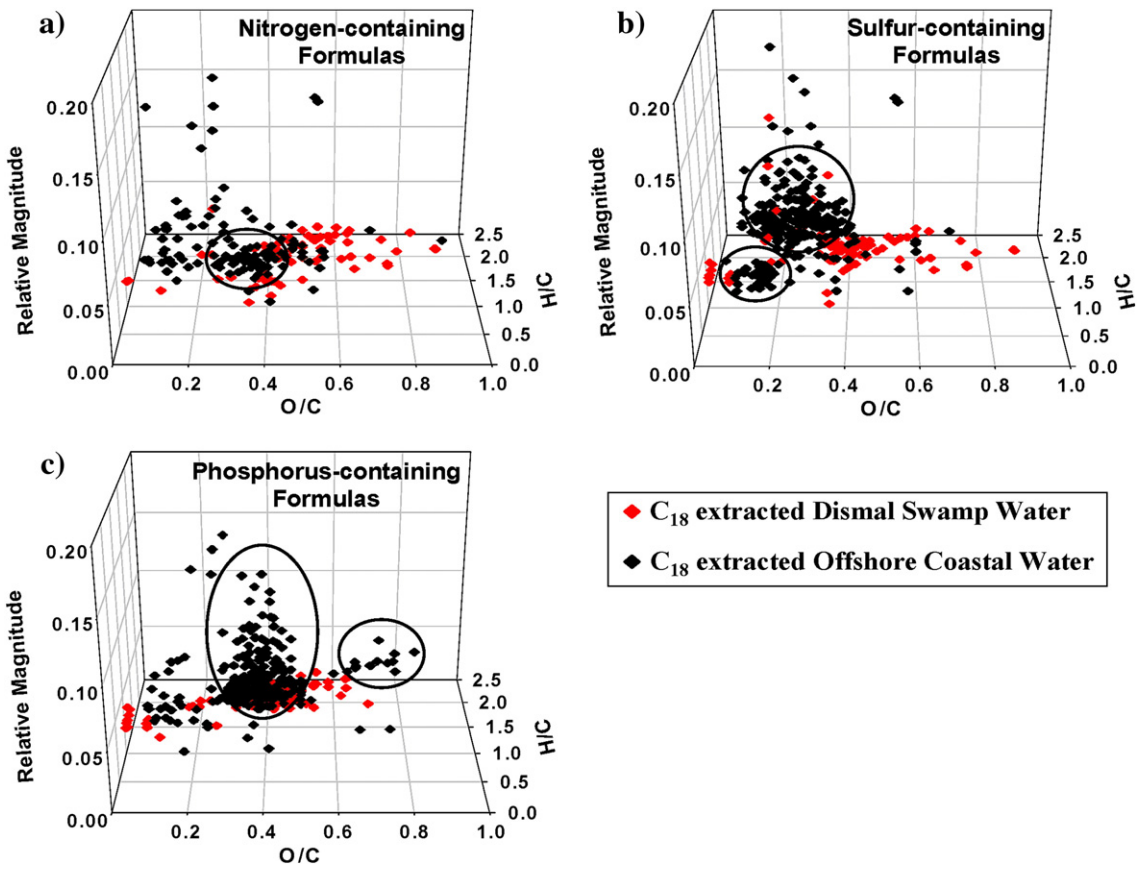

Fig. 9. The three dimensional van Krevelen diagrams of the formulas containing nitrogen (a), sulfur (b), and phosphorus (c) for the C_{18} extracted Dismal Swamp water (red points) and the C_{18} extracted offshore coastal water (black points). The *z*-axis is the relative peak magnitudes (percent of the summed total magnitude of all peaks).

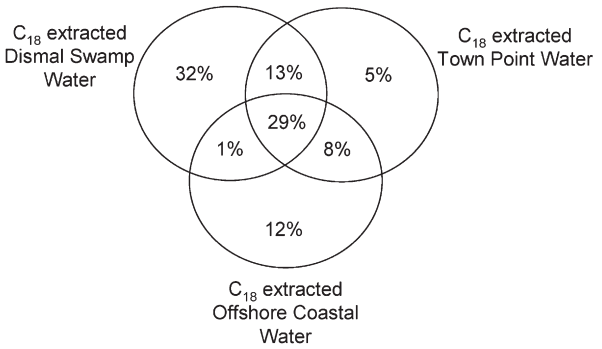

Fig. 10. The Venn diagram of the C_{18} extracted Dismal Swamp, Town Point, and offshore coastal waters. Percentages in areas of overlap are percentages of molecular formulas that appear in both (or all three) of those samples. Percentages in areas with no overlap are of molecular formulas that are unique to that individual sample.

Recently, a new parameter for DOM characterization has been proposed by Koch et al. (2005). This parameter, DBE−O, is obtained from the molecular formula by subtracting the number of oxygens in the formula from the double bond equivalent. It has been suggested that this parameter provides information about the degree of unsaturation or ring closure for only the backbone carbon structure by eliminating the effect oxygen has on DBE by assuming that it exists only as doubly bound oxygen in carbonyl groups (Koch et al., 2005; Dittmar and Koch, 2006; Tremblay et al., 2007). However, this assumption may not be appropriate, especially for lignin-like structures, because oxygens in alcohol and ether groups, as well as the C–O–C oxygens in esters and the hydroxyl oxygens in carboxylic acids, are not double bonded. This DBE−O parameter has been utilized in an attempt to distinguish between DOM samples with moderately oxygenated, lower DBE molecules from those with a larger number of unsaturations that are likely condensed aromatics. Low (i.e., more negative) values of DBE−O indicate molecules that are more oxygenated, while high (i.e., more positive) values indicate more unsaturated, condensed aromatics. For this transect, DBE−O was determined for each molecular formula in all of the samples, and then histogram plots of the frequency for each DBE−O value were constructed. The distribution of DBE−O values showed no significant changes between samples. The same unimodal range of DBE−O values from −12 to +14 existed in all samples, with the highest frequency occurring between −1 and +1. The fact that this DBE−O parameter is invariant for this sample set indicates that either onshore and offshore DOM share the same DBE−O characteristics or that the parameter does not provide adequate sensitivity for changes in molecular composition. Considering the significant changes observed in the spectral features, we suggest that this DBE−O parameter is not very useful for this data set because it ignores sp^3 oxygen likely to be an important component of lignin-derived DOM.

3.4. Terrestrial DOM export to the ocean

From Fig. 7, it is apparent that the molecular formulas for the multitude of peaks in FTICR mass spectra of coastal DOM overlap significantly with those from the Dismal Swamp DOM in the lignin region of the VK diagram. Stenson et al. (2003) speculated that a large proportion of peaks in riverine fulvic acid could be attributed to lignin-derived species and presented a lignin degradation pathway explaining how lignin degradation products are incorporated into the organic matter matrix. It appears logical that such a high degree of overlap, coupled with the belief that lignin is the main component of DOM in coastal swamp systems like the Okefenokee Swamp (source of Suwannee River DOM) and the Dismal Swamp examined in this study, indicates that lignin is making its way out into offshore Chesapeake Bay waters in significant amounts. In another FTICR-MS study focused on the source of marine DOM, Koch et al. (2005) determined that approximately one-third of assigned molecular formulas were common to samples emanating from mangrove swamps in coastal Brazil and oceanic samples off the coast of Antarctica. This is consistent with our findings and the Venn diagram presented in Fig. 10.

Estimates of the amounts of lignin in oceanic DOM, based on lignin signatures characteristic of terrestrial plants, indicate that lignin contributes to less than 2.4% of the total oceanic DOM (Opsahl and Benner, 1997). Mitra et al. (2000) observed similar low values for lignin phenols in the Middle Atlantic Bight, near the offshore station examined in this study. However, the invasive method used for isolating lignin phenols (CuO oxidation) may underestimate the actual amount of terrestrial organic matter in the ocean, especially if biodegradation or photodegradation alters the DOM. This is especially true if, for example, a lignin compound is modified such that its structure no longer contains the methoxy aromatic phenols that are used as proxies for lignin in the CuO method. Demethylation or replacement of a methoxyl group with a hydroxyl group (an important biodegradation reaction) and ring-opening reactions (photochemical degradation reactions) would not significantly alter the location of a compound on the VK diagram. Thus, such reactions would change the compound but not to the point where it would be labeled a non-lignin compound by FTICR-MS. However, such changes would eliminate its consideration as a lignin phenol by the CuO method.

One central question still remains unanswered: Do the overlapping peaks in the lignin region of the VK diagram have the same molecular structure, or simply the same molecular formula but with different structures? Fig. 11 shows a lignin model structure and a representative CRAM (carboxyl rich alicyclic molecule) model structure, which are two structural isomers for $C_{26}H_{32}O_{11}$. CRAM structures have been proposed as a

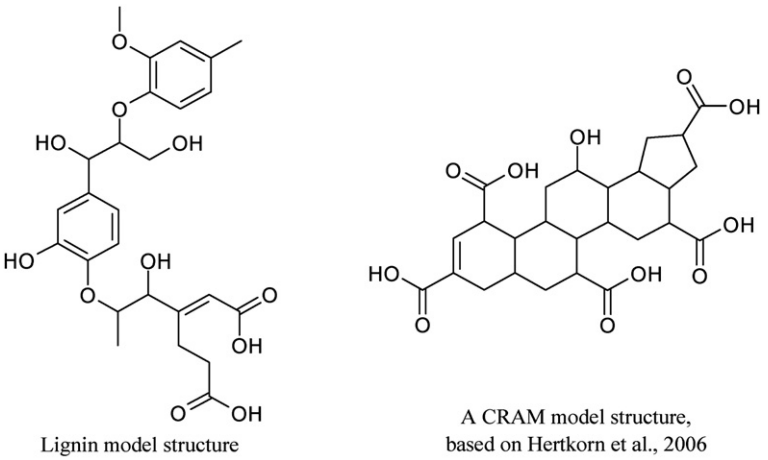

Fig. 11. Two structural isomers of the same molecular formula, $C_{26}H_{32}O_{11}$. One is a lignin model structure and the other is a CRAM (Carboxyl Rich Alicyclic Molecules) model structure, (Hertkorn et al., 2006).

major refractory component of marine DOM (Hertkorn et al., 2006; Hertkorn et al., 2007), but more recently CRAM has been proposed as a component of freshwater DOM as well (Lam et al., 2007). It is possible that these are the types of structures that are present in marine samples as opposed to lignin-derived structural entities present in more riverine samples. Although these two structures have the same formula and plot in the same area of the VK diagram, they have different reactivities and sources. Further experiments need to be performed on these samples to confidently assign a distinct origin to peaks in the "lignin" region of the VK plot. Further evidence for the existence of significant terrestrial DOM in the coastal ocean off the Chesapeake Bay comes from fatty acids that are identified in the coastal DOM. Saturated fatty acids with carbon chains in the range of C_{14}–C_{26} are detected in the offshore coastal DOM sample. The higher carbon numbered fatty acids are biomarkers for terrestrial plants (Mannino and Harvey, 1999; Mannino and Harvey, 2000). While the shorter chained fatty acids ($<C_{23}$) do not exclusively point to a vascular plant source, Mannino and Harvey (2000) speculated that they did.

4. Conclusions

ESI-FTICR-MS is clearly a powerful technique for the examination of the complex composition of DOM along this river to ocean transect of the lower Chesapeake Bay. It not only has the capacity to resolve the thousands of components in DOM, but also its low detection limit allows, for the first time, the direct infusion and analysis of a whole water sample without any prior concentration or fractionation. The Dismal Swamp whole water contains two sets of compounds that are excluded when using the C_{18} extraction protocol: one in the tannin region and one in the aliphatic amine/amide region. Clearly, a more complete characterization of any DOM sample can only be accomplished when no selective fractionation occurs. Visualization tools, such as the VK diagram, highlight the spatial variations that occur between DOM samples. A shift from more aromatic, terrestrial DOM to more aliphatic, marine DOM can be clearly observed as sampling progress offshore. The DOM also becomes more structurally diverse offshore as the number of N, S, and P-containing compounds increases. As the terrestrial DOM is exported to the open ocean, O/C values initially decrease and then level off while H/C values continuously increase and DBE values decrease. Mechanisms such as photochemistry or microbial processes could likely be responsible for these types of aromatic to aliphatic DOM transformations and structural reworkings. Although each sample along the transect possesses a certain amount of unique molecular formulas, each sample also overlaps quite significantly with other sites. The remarkable degree of overlap of peaks centered in the lignin region of the VK diagram suggests that lignin may be a more significant source of the DOM structures observed than has previously been considered based on CuO biomarker analyses. While this study focused on one particular estuarine system, the lower Chesapeake Bay, it is a system that is considered representative of many estuaries worldwide. The processes and mechanisms that were investigated here should be generally applicable across many aquatic environments.

Acknowledgements

We thank Hussain Abdulla for his assistance in sample collection and laboratory measurements, Susan Hatcher at the COSMIC (College of Sciences Major Instrumentation Cluster) facility at Old Dominion University for her assistance with the FTICR-MS analyses, and the crew of the R/V Fay Slover. We thank Dr. Zhanfei Liu for providing useful discussions on DOM characterization and transport. We also thank the anonymous reviewers, whose comments significantly improved the quality of this manuscript. This work was funded by the National Science Foundation Chemical Oceanography Program, grant number OCE-0612712.

References

Akkanen, J., Kukkonen, J.V.K., 2003. Measuring the bioavailability of two hydrophobic organic compounds in the presence of dissolved organic matter. Environmental Toxicology and Chemistry 22 (3), 518–524.

Akkanen, J., Vogt, R.D., Kukkonen, J.V.K., 2004. Essential characteristics of natural dissolved organic matter affecting the sorption of hydrophobic organic contaminants. Aquatic Sciences 66 (2), 171–177.

Arzayus, K.M., Canuel, E.A., 2004. Organic matter degradation in sediments of the York River estuary: effects of biological vs. physical mixing. Geochimica et Cosmochimica Acta 69 (2), 455–463.

Bianchi, T.S., Lambert, C.D., Santschi, P.H., Laodong, G., 1997. Sources and transport of land-derived particulate and dissolved organic matter in the Gulf of Mexico (Texas shelf/slope): the use of lignin-phenols and loliolides as biomarkers. Organic Geochemistry 27 (1), 65–78.

Boehme, J., Wells, M., 2006. Fluorescence variability of marine and terrestrial colloids: examining size fractions of chromophoric dissolved organic matter in the Damariscotta river estuary. Marine Chemistry 101 (1–2), 95–103.

Boyd, T.J., Osburn, C.L., 2004. Changes in CDOM fluorescence from allochthonous and autochthonous sources during tidal mixing and bacterial degradation in two coastal estuaries. Marine Chemistry 89 (1), 189–210.

Brown, T.L., Rice, J.A., 2000. Effect of experimental parameters on the ESI FT-ICR mass spectrum of fulvic acid. Analytical Chemistry 72 (2), 384–390.

Burdige, D.J., 2001. Dissolved organic matter in Chesapeake Bay sediment pore waters. Organic Geochemistry 32 (4), 487–505.

Burdige, D.J., Kline, S.W., Chen, W., 2004. Fluorescent dissolved organic matter in marine sediment pore waters. Marine Chemistry 89 (1), 289–311.

Chen, M., Wang, W.X., Guo, L., 2004. Phase partitioning and solubility of iron in natural seawater controlled by dissolved organic matter. Global Biogeochemical Cycles 18 (4), GB4013.

Chiou, C.T., Malcolm, R.L., Brinton, T.I., Kile, D.E., 1986. Water solubility enhancement of some organic pollutants and pesticides by dissolved humic and fulvic acids. Environmental Science and Technology 20 (5), 502–508.

Chiou, C.T., Kile, D.E., Brinton, T.I., Malcolm, R.L., Leenheer, J.A., MacCarthy, P., 1987. A comparison of water solubility enhancements of organic solutes by aquatic humic materials and commercial humic acids. Environmental Science and Technology 21 (12), 1231–1234.

Coble, P.G., 1996. Characterization of marine and terrestrial DOM in seawater using excitation-emission matrix spectroscopy. Marine Chemistry 51 (4), 325–346.

Countway, R.E., Canuel, E.A., Dickhut, R.M., 2007. Sources of particulate organic matter in surface waters of the York River, VA estuary. Organic Geochemistry 38 (3), 365–379.

De Leeuw, J.W., Largeau, C., 1993. A review of macromolecular organic compounds that comprise living organisms and their role in kerogen, coal, and petroleum formation. In: Engel, M.H., Macko, S.A. (Eds.), Organic Geochemistry: Principles and Practice. Plenum Press, New York, pp. 23–72.

Dittmar, T., Koch, B.P., 2006. Thermogenic organic matter dissolved in the abyssal ocean. Marine Chemistry 102 (3–4), 208–217.

Drexel, R.T., Haitzer, M., Ryan, J.N., Aiken, G.R., Nagy, K.L., 2002. Mercury (II) sorption to two Florida Everglades peats: evidence for strong and weak binding and competition by dissolved organic matter released from the peat. Environmental Science and Technology 36 (19), 4058–4064.

Frazier, S.W., Kaplan, L.A., Hatcher, P.G., 2005. Molecular characterization of biodegradable dissolved organic matter using bioreactors and [12 C/13 C] tetramethylammonium hydroxide thermochemolysis GC-MS. Environmental Science and Technology 39 (6), 1479–1491.

Fukushima, M., Tanabe, Y., Yabuta, H., Tanaka, F., Ichikawa, H., Tatsumi, K., Watanabe, A., 2006. Water solubility enhancement effects of some polychlorinated organic pollutants by dissolved organic carbon from a soil with a higher organic carbon content. Journal of Environmental Science and Health, Part A: Toxic/Hazardous Substances & Environmental Engineering 41 (8), 1483–1494.

Gaskell, S.J., 1997. Electrospray: principles and practice. Journal of Mass Spectrometry 32 (7), 677–688.

Gourlay, C., Tusseau-Vuillemin, M.H., Mouchel, J.M., Garric, J., 2005. The ability of dissolved organic matter (DOM) to influence benzo [a] pyrene bioavailability increases with DOM biodegradation. Ecotoxicology and Environmental Safety 61 (1), 74–82.

Hedges, J.I., 1992. Global biogeochemical cycles: progress and problems. Marine Chemistry 39 (1–3), 67–93.

Hedges, J.I., 2002. Why dissolved organics matter? In: Hansell, D.A., Carlson, C.A. (Eds.), Biogeochemistry of Marine Dissolved Organic Matter. Academic Press, Boston, pp. 1–33.

Hedges, J.I., Keil, R.G., Benner, R., 1997. What happens to terrestrial organic matter in the ocean? Organic Geochemistry 27 (5), 195–212.

Henriksen, T., Juhler, R.K., Svensmark, B., Cech, N.B., 2005. The relative influences of acidity and polarity on responsiveness of small organic molecules to analysis with negative ion electrospray ionization mass spectrometry (ESI-MS). Journal of the American Society for Mass Spectrometry 16 (4), 446–455.

Hertkorn, N., Benner, R., Frommberger, M., Schmitt-Kopplin, P., Witt, M., Kaiser, K., Kettrup, A., Hedges, J.I., 2006. Characterization of a major refractory component of marine dissolved organic matter. Geochimica et Cosmochimica Acta 70, 2990–3010.

Hertkorn, N., Ruecker, C., Meringer, M., Gugisch, R., Frommberger, M., Perdue, E. M., Witt, M., Schmitt-Kopplin, P., 2007. High-precision frequency measurements: indispensable tools at the core of the molecular-level analysis of complex systems. Analytical and Bioanalytical Chemistry 389 (5), 1311–1327.

Hockaday, W.C., Grannas, A.M., Kim, S., Hatcher, P.G., 2006. Direct molecular evidence for the degradation and mobility of black carbon in soils from ultrahigh-resolution mass spectral analysis of dissolved organic matter from a fire-impacted forest soil. Organic Geochemistry 37 (4), 501–510.

Hopkinson, C.S., Buffam, I., Hobbie, J., Vallino, J., Perdue, M., Eversmeyer, B., Prahl, F., Covert, J., Hodson, R., Moran, M.A., 1998. Terrestrial inputs of organic matter to coastal ecosystems: an intercomparison of chemical characteristics and bioavailability. Biogeochemistry 43 (3), 211–234.

Johannesson, K.H., Tang, J., Daniels, J.M., Bounds, W.J., Burdige, D.J., 2004. Rare earth element concentrations and speciation in organic-rich blackwaters of the Great Dismal Swamp, Virginia, USA. Chemical Geology 209 (3–4), 271–294.

Kaiser, E., Simpson, A.J., Dria, K.J., Sulzberger, B., Hatcher, P.G., 2003. Solid-state and multidimensional solution-state NMR of solid phase extracted and ultrafiltered riverine dissolved organic matter. Environmental Science and Technology 37 (13), 2929–2935.

Kendrick, E., 1963. A mass scale based on CH2 = 14.0000 for high resolution mass spectrometry of organic compounds. Analytical Chemistry 35 (13), 2146–2154.

Kim, S., Kramer, R.W., Hatcher, P.G., 2003a. Graphical method for analysis of ultrahigh-resolution broadband mass spectra of natural organic matter, the van Krevelen diagram. Analytical Chemistry 75 (20), 5336–5344.

Kim, S., Simpson, A.J., Kujawinski, E.B., Freitas, M.A., Hatcher, P.G., 2003b. High resolution electrospray ionization mass spectrometry and 2D solution NMR for the analysis of DOM extracted by C18 solid phase disk. Organic Geochemistry 34 (9), 1325–1335.

Kim, S., Kaplan, L.A., Benner, R., Hatcher, P.G., 2004. Hydrogen-deficient molecules in natural riverine water samples — evidence for the existence of black carbon in DOM. Marine Chemistry 92 (1), 225–234.

Kim, S., Kaplan, L.A., Hatcher, P.G., 2006. Biodegradable dissolved organic matter in a temperate and a tropical stream determined from ultra-high resolution mass spectrometry. Limnology and Oceanography 51 (2), 1054–1063.

Koch, B.P., Witt, M., Engbrodt, R., Dittmar, T., Kattner, G., 2005. Molecular formulae of marine and terrigenous dissolved organic matter detected by electrospray ionization Fourier transform ion cyclotron resonance mass spectrometry. Geochimica et Cosmochimica Acta 69 (13), 3299–3308.

Kramer, R.W., Kujawinski, E.B., Hatcher, P.G., 2004. Identification of black carbon derived structures in a volcanic ash soil humic acid by Fourier transform ion cyclotron resonance mass spectrometry. Environmental Science and Technology 38 (12), 3387–3395.

Kujawinski, E.B., Behn, M.D., 2006. Automated analysis of electrospray ionization Fourier transform ion cyclotron resonance mass spectra of natural organic matter. Analytical Chemistry 78 (13), 4363–4373.

Kujawinski, E.B., Freitas, M.A., Zang, X., Hatcher, P.G., Green-Church, K.B., Jones, R.B., 2002. The application of electrospray ionization mass spectrometry (ESI MS) to the structural characterization of natural organic matter. Organic Geochemistry 33 (3), 171–180.

Kujawinski, E.B., Del Vecchio, R., Blough, N.V., Klein, G.C., Marshall, A.G., 2004. Probing molecular-level transformations of dissolved organic matter: insights on photochemical degradation and protozoan modification of DOM from electrospray ionization Fourier transform ion cyclotron resonance mass spectrometry. Marine Chemistry 92 (1–4), 23–37.

Lam, B., Baer, A., Alaee, M., Lefebvre, B., Moser, A., Williams, A., Simpson, A.J., 2007. Major structural components in freshwater dissolved organic matter. Environmental Science & Technology 41 (24), 8240–8247.

Lichter, W.F., Walker, P.N., 1979. Hydrology of the Dismal Swamp, Virginia-North Carolina. In: KirkJr. Jr., P.W. (Ed.), The Great Dismal Swamp. Univ. Press of Virginia, Charlottesville, pp. 140–168.

Llewelyn, J.M., Landing, W.M., Marshall, A.G., Cooper, W.T., 2002. Electrospray ionization Fourier transform ion cyclotron resonance mass spectrometry of dissolved organic phosphorus species in a treatment wetland after selective isolation and concentration. Analytical Chemistry 74 (3), 600–606.

Louchouarn, P., Opsahl, S., Benner, R., 2000. Isolation and quantification of dissolved lignin from natural waters using solid-phase extraction and GC/MS. Analytical Chemistry 72 (13), 2780–2787.

Maie, N., ChengYong, Y., Miyoshi, T., Parish, K., Jaffe, R., 2005. Chemical characteristics of dissolved organic matter in an oligotrophic subtropical wetland/estuarine ecosystem. Limnology and Oceanography 50 (1), 23–35.

Mannino, A., Harvey, H.R., 1999. Lipid composition in particulate and dissolved organic matter in the Delaware Estuary: sources and diagenetic patterns — Observation. Geochimica et Cosmochimica Acta 63 (15), 2219–2235.

Mannino, A., Harvey, H.R., 2000. Terrigenous dissolved organic matter along an estuarine gradient and its flux to the coastal ocean. Organic Geochemistry 31 (12), 1611–1625.

Marshall, A.G., Hendrickson, C.L., Jackson, G.S., 1998. Fourier transform ion cyclotron resonance mass spectrometry: a primer. Mass Spectrometry Reviews 17 (1), 1–35.

McCallister, S.L., Bauer, J.E., Ducklow, H.W., Canuel, E.A., 2006. Sources of estuarine dissolved and particulate organic matter: a multi-tracer approach. Organic Geochemistry 37 (4), 454–468.

Meunier, L., Laubscher, H., Hug, S.J., Sulzberger, B., 2005. Effects of size and origin of natural dissolved organic matter compounds on the redox cycling of iron in sunlit surface waters. Aquatic Sciences 67 (3), 292–307.

Meyers-Schulte, K.J., Hedges, J.I., 1986. Molecular evidence for a terrestrial component of organic matter dissolved in ocean water. Nature 321 (6065), 61–63.

Minor, E.C., Nallanthamby, P.S., 2004. "Cellular" vs. "Detrital" POM: a preliminary study using fluorescent stains, flow cytometry, and mass spectrometry. Marine Chemistry 92 (1–4), 9–21.

Minor, E.C., Boon, J.J., Harvey, H.R., Mannino, A., 2001. Estuarine organic matter composition as probed by direct temperature-resolved mass spectrometry and traditional geochemical techniques. Geochimica et Cosmochimica Acta 65 (17), 2819–2834.

Minor, E.C., Simjouw, J.P., Boon, J.J., Kerkhoff, A.E., van der Horst, J., 2002. Estuarine/marine UDOM as characterized by size-exclusion chromatography and organic mass spectrometry. Marine Chemistry 78 (2), 75–102.

Minor, E.C., Pothen, J., Dalzell, B.J., Abdulla, H., Mopper, K., 2006. Effects of salinity changes on the photodegradation and ultraviolet–visible absorbance of terrestrial dissolved organic matter. Limnology and Oceanography 51 (5), 2181–2186.

Mitra, S., Bianchi, T.S., Guo, L., Santschi, P.H., 2000. Terrestrially derived dissolved organic matter in the Chesapeake Bay and the Middle Atlantic Bight. Geochimica et Cosmochimica Acta 64 (20), 3547–3557.

Nanny, M.A., Maza, J.P., 2001. Noncovalent interactions between monoaromatic compounds and dissolved humic acids: a deuterium NMR T 1 relaxation study. Environmental Science and Technology 35 (2), 379–384.

Nanny, M.A., Bortiatynski, J.M., Hatcher, P.G., 1997. Noncovalent interactions between acenaphthenone and dissolved fulvic acid as determined by 13C NMR T1 relaxation measurements. Environmental Science and Technology 31 (2), 530–534.

Nelson, D.L., Cox, M.M., 2000a. Carbohydrates and glycobiology. In: Ryan, M. (Ed.), Principles of Biochemistry. Worth, New York, pp. 293–324.

Nelson, D.L., Cox, M.M., 2000b. Lipids. In: Ryan, M. (Ed.), Principles of Biochemistry. Worth, New York, pp. 363–388.

Opsahl, S., Benner, R., 1997. Distribution and cycling of terrigenous dissolved organic matter in the ocean. Nature 386 (6624), 480–482.

Reemtsma, T., These, A., Linscheid, M., Leenheer, J., Spitzy, A., 2008. Molecular and structural characterization of dissolved organic matter from the deep ocean by FTICR-MS, including hydrophilic nitrogenous organic molecules. Environmental Science and Technology 42 (5), 1430–1437.

Repeta, D.J., Quan, T.M., Aluwihare, L.I., Accardi, A., 2002. Chemical characterization of high molecular weight dissolved organic matter in fresh and marine waters. Geochimica et Cosmochimica Acta 66 (6), 955–962.

Rochelle-Newall, E.J., Fisher, T.R., 2002. Chromophoric dissolved organic matter and dissolved organic carbon in Chesapeake Bay. Marine Chemistry 77 (1), 23–41.

Rostad, C.E., Leenheer, J.A., 2004. Factors that affect molecular weight distribution of Suwannee river fulvic acid as determined by electrospray ionization/mass spectrometry. Analytica Chimica Acta 523 (2), 269–278.

Santschi, P.H., Lenhart, J.J., Honeyman, B.D., 1997. Heterogeneous processes affecting trace contaminant distribution in estuaries: the role of natural organic matter. Marine Chemistry 58 (1), 99–125.

Sholkovitz, E.R., 1978. The flocculation of dissolved Fe, Mn, Al, Cu, Ni, Co and Cd during estuarine mixing. Earth and Planetary Science Letters 41 (1), 77–86.

Sholkovitz, E.R., Copland, D., 1981. The coagulation, solubility and adsorption properties of Fe, Mn, Cu, Ni, Cd, Co and humic acids in a river water. Geochimica et Cosmochimica Acta 45 (2), 181–189.

Sholkovitz, E.R., Boyle, E.R., Price, N.B., 1978. Removal of dissolved humic acid and iron during estuarine mixing. Earth and Planetary Science Letters 40 (1), 130–136.

Simpson, M.J., Simpson, A.J., Hatcher, P.G., 2004. Noncovalent interactions between aromatic compounds and dissolved humic acid examined by nuclear magnetic resonance spectroscopy. Environmental Toxicology and Chemistry 23 (2), 355–362.

Sleighter, R.L., Hatcher, P.G., 2007. The application of electrospray ionization coupled to ultrahigh resolution mass spectrometry for the molecular characterization of natural organic matter. Journal of Mass Spectrometry 42 (5), 559–574.

Sleighter, R.L., McKee, G.A., Liu, Z., Hatcher, P.G., 2008. Naturally present fatty acids as internal calibrants for Fourier transform mass spectra of dissolved organic matter. Limnology and Oceanography: Methods 6.

Slowey, J.F., Jeffrey, L.M., Hood, D.W., 1962. The fatty-acid content of ocean water. Geochimica et Cosmochimica Acta 26 (6), 607–616.

Stenson, A.C., Landing, W.M., Marshall, A.G., Cooper, W.T., 2002. Ionization and fragmentation of humic substances in electrospray ionization Fourier transform-ion cyclotron resonance mass spectrometry. Analytical Chemistry 74 (17), 4397–4409.

Stenson, A.C., Marshall, A.G., Cooper, W.T., 2003. Exact masses and chemical formulas of individual Suwannee River fulvic acids from ultrahigh resolution electrospray ionization Fourier transform ion cyclotron resonance mass spectra. Analytical Chemistry 75 (6), 1275–1284.

Traina, S.J., McAvoy, D.C., Versteeg, D.J., 1996. Association of linear alkylbenzenesulfonates with dissolved humic substances and its effect on bioavailability. Environmental Science and Technology 30 (4), 1300–1309.

Tremblay, L.B., Dittmar, T., Marshall, A.G., Cooper, W.J., Cooper, W.T., 2007. Molecular characterization of dissolved organic matter in a North Brazilian mangrove-fringed estuary by FT-ICR mass spectrometry and synchronous fluorescence spectroscopy. Marine Chemistry 105 (1–2), 15–29.

van Krevelen, D., 1950. Graphical-statistical method for the study of structure and reaction process of coal. Fuel 29, 269–284.

Williams, P.M., Druffel, E.R.M., 1987. Radiocarbon in dissolved organic matter in the central North Pacific Ocean. Nature 330 (6145), 246–248.

Zimmerman, A.R., Canuel, E.A., 2000. A geochemical record of eutrophication and anoxia in Chesapeake Bay sediments: anthropogenic influence on organic matter composition. Marine Chemistry 69 (1), 117–137.